

# Continuous vs. Discrete Models of Nonadiabatic Monolith Catalysts

Gianpiero Groppi and Enrico Tronconi

Dip. di Chimica Industriale e Ingegneria Chimica, Politecnico di Milano, 20133 Milano, Italy

Monolith catalysts are widely applied for clean up of waste gases [catalytic mufflers, volatile organic compound (VOC) incinerators, reactors for selective catalytic reduction (SCR) of  $\text{NO}_x$  by  $\text{NH}_3$ ] in view of their unique combination of low-pressure drops and high gas–solid interfacial areas. Literature studies on the use of monolith catalysts in chemical process applications have been recently reviewed (Cybulski and Moulijn, 1994a). A growing interest is now becoming apparent in the use of monoliths as catalysts in nonadiabatic reactors because of their favorable global heat-transfer properties resulting from the connected structure of the solid matrix.

Most of the existing mathematical models of monolith catalysts refer to reactors operating under isothermal (SCR of  $\text{NO}_x$ ) or adiabatic (catalytic combustion) conditions. In these cases, assuming an ideally uniform distribution of the inlet variables, simulation of a single channel is representative of the behavior of the whole monolith. On the other hand, thermal interactions between the channels have to be accounted for to predict the effects of nonuniform distributions of the inlet variables and, of course, in the simulation of externally cooled or heated reactors. Very few articles in the literature (Flytzani-Stephanopoulos et al., 1986; Kolackowski et al., 1988; Cybulski and Moulijn, 1994b; Tronconi et al., 1995) have addressed the analysis of heat transfer in nonadiabatic monolithic reactors, all of them adopting discrete models of the monolith structure. Such models are based on a discretization of the temperature (and concentration) profiles within the monolith matrix, which is strictly related to the monolith cell, that is, the base element of its structure. Usually the monolith geometry is reconfigured by arranging the channels in  $N$  coaxial rings to secure circular symmetry, which is computationally advantageous (Kolackowski et al., 1988). Moreover, when dealing with complex channel geometries (e.g., sinusoidal cells in metallic monoliths), the cross section of the single channels is also approximated by simpler shapes such as square (Flytzani-Stephanopoulos et al., 1986; Kolackowski et al., 1988) or triangle (Cybulski and Moulijn, 1994b). Enthalpy balance equations are then written for each element of the discretized, reconfigured matrix, and heat fluxes within the solid walls are calculated by a finite differ-

ence approximation using a mesh of constant grid size that is intrinsically associated with the annular reconfigured geometry. Despite the reconfiguration, this approach is numerically expensive when dealing with monolith matrices exhibiting large global-to-channel-size ratios (i.e., with several channel “rings”), which are, however, common in practical applications. Moreover, the reconfiguration of the monolith modifies its geometrical parameters, which in turn may adversely affect prediction of the monolith performances (Cybulski and Moulijn, 1994b).

Continuous models of the monolith matrix provide an interesting alternative. Mathematical models based on a continuum approach represent well-established and classic tools for the analysis and design of packed-bed tubular reactors. Continuous models using Hahn polynomials as approximants in a collocation scheme were used to represent discrete multistaged separators (Stewart et al., 1985). Indeed, a continuum approximation of the monolith matrix appears to be legitimate in principle when the dimensions of the microscale (single channel) and of the macroscale (monolith matrix) differ by orders of magnitude. In this case, accordingly, a local interspersed of gas and solid can be assumed, along with a continuous distribution of variables within the two phases. For monoliths, this class of models was first proposed by Aris (1979), who also proved the mathematical equivalence of the solutions of continuous and discrete models in the limit of the microscale dimension approaching zero. The crucial point in continuous heat-transfer models is the evaluation of the effective thermal conductivity coefficients, which are functions both of the physical properties of the two phases and of the monolith geometry. To our knowledge only one expression has been proposed in the literature for calculation of such coefficients (Liu, 1975; Zygorakis, 1989). However, this expression provides asymptotic values of the radial effective conductivity, which are not physically consistent in the limits  $\epsilon \rightarrow 0$  and  $\epsilon \rightarrow 1$ .

In this work a novel expression for calculation of the radial effective conductivity is derived. The physical consistency of the steady-state continuous model implementing such an expression is then analyzed by comparison with a discrete monolith model. In spite of the just-mentioned limitations, discrete models have been partially validated in the literature

Correspondence concerning this article should be addressed to E. Tronconi.

against experimental temperature profiles in heated monoliths; thus, they can be regarded as a standard in evaluating the adequacy of the continuum approach. The reference problem of pure heat transfer with constant temperature of the external monolith wall is investigated for these purposes.

## Model Development

In this work the discrete and continuous models of the monolith matrix have been derived under the following common assumptions: (1) pure heat transfer (no chemical reaction) with set uniform temperature of the external monolith wall; (2) steady-state conditions; (3) cylindrical monolith with square channels; (4) gas-phase balance equation written under a one-dimensional (1-D) approximation of the monolith channels, with gas-solid heat-transfer coefficients derived from correlations in the literature for fully developed laminar flow (Grigull and Tratz, 1965); (5) negligible axial heat conduction in the gas phase; (6) negligible heat transfer by radiation; (7) negligible pressure drop; (8) temperature-dependent gas (air) properties; and (9) uniform velocity distribution over the monolith cross section. Although nonuniform velocity distributions may actually occur in monolithic catalysts under practical conditions, it can be reasonably assumed that they have negligible effects within the aim of the present work.

### Continuous model

Continuous monolith models assume that gas and solid phases are locally and uniformly interspersed. For the heat-transfer problem herein investigated, such models consist of enthalpy balances for the two phases derived assuming a segregated gas phase exchanging heat with a thermally connected solid matrix that in turn interacts with the external heating or cooling medium. Model equations are written in the following in dimensionless form, with symbols explained in the Notation section.

Gas phase:

$$Pe' \cdot \frac{\partial T^*}{\partial z^*} = 4 \cdot Nu \cdot L^* \cdot (W^* - T^*). \quad (1)$$

Solid phase:

$$k_{as}^* \cdot \left( \frac{1}{L^*} \right)^2 \cdot \frac{\partial^2 W^*}{\partial z^{*2}} + 4 \cdot k_{rs}^* \cdot \left( \frac{1}{D^*} \right)^2 \cdot \left( \frac{\partial^2 W^*}{\partial r^{*2}} + \frac{1}{r^*} \cdot \frac{\partial W^*}{\partial r^*} \right) + 4 \cdot Nu \cdot (T^* - W^*) = 0. \quad (2)$$

Inlet conditions ( $z^* = 0$ ):

$$T^*(0, r^*) = 1, \quad \frac{\partial W^*}{\partial z^*}(0, r^*) = 0. \quad (3,4)$$

Symmetry condition at the monolith axis ( $r^* = 0$ ):

$$\frac{\partial W^*}{\partial r^*}(z^*, 0) = 0. \quad (5)$$

Outlet condition ( $z^* = 1$ ):

$$\frac{\partial W^*}{\partial z^*}(1, r^*) = 0. \quad (6)$$

Boundary condition at the monolith wall ( $r^* = 1$ ):

$$W^*(z^*, 1) = T_{\text{ext}}^*. \quad (7)$$

Evaluation of the effective axial and radial conductivity coefficients ( $k_{as}$  and  $k_{rs}$ ) is the crucial point in the development of continuous models of the monolith matrix. Considering the parallel flow pattern in the monolith matrix, the following expression is easily derived for the axial effective conductivity:  $k_{as} = (1 - \epsilon) \cdot k_s$ .

Derivation of the effective radial conductivity is more complex. Monoliths can be regarded as periodic structures originated by the repetition of elementary unit cells. The basic idea is that the effective radial conductivity coefficients of the whole cross section can be derived from the analysis of the heat-transfer mechanism in the elementary unit cell. Note that this approach resembles the one usually adopted for the evaluation of effective heat-transfer parameters in packed beds (Bauer and Schlunder, 1978), the difference being that in packed beds the unit cell is defined on a statistical basis, while in monolith catalysts it corresponds to a real element of the periodic structure.

Let us consider the monolith element reported in Figure 1a as the projection of the elementary cell on the cross-sectional plane, and assume a unit length along the axial di-

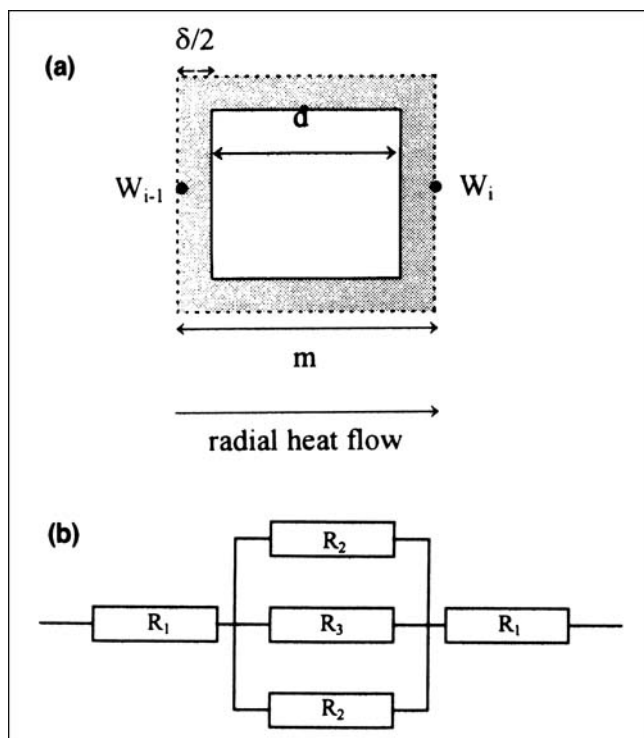


Figure 1. (a) Unit cell projection on the cross-sectional plane of a square-cell monolith; (b) equivalent thermal-resistance scheme.

rection. For a uniform temperature difference at the boundary along the radial direction, heat flows across the cell by conduction both in the solid phase and in the gas phase. Neglecting radiative contributions, the resistance scheme plotted in Figure 1b can be assumed, where the single resistances are easily computed according to the classic theory of heat conduction in solids. Thus,

$$R_1 = \frac{1}{k_s} \cdot \frac{\delta}{2 \cdot m \cdot 1}; \quad (8)$$

$$R_2 = \frac{1}{k_s} \cdot \frac{2 \cdot d}{\delta \cdot 1}; \quad (9)$$

$$R_3 = \frac{1}{k_g} \cdot \frac{d}{d \cdot 1}. \quad (10)$$

By in-parallel-in-series combination the overall equivalent resistance to heat transfer across the unit cell can be evaluated as

$$R_c = 2 \cdot R_1 + \frac{R_2/2 \cdot R_3}{R_2/2 + R_3} = \frac{1}{k_s \cdot 1} \cdot \left( 1 - \sqrt{\epsilon} + \frac{1}{\frac{k_g}{k_s} + \left( \frac{1 - \sqrt{\epsilon}}{\sqrt{\epsilon}} \right)} \right), \quad (11)$$

and eventually the following expression for  $k_{rs}$  is derived:

$$k_{rs} = R_c^{-1} \cdot \frac{s_c}{A_c} = \frac{k_s}{1 - \sqrt{\epsilon} + \frac{1}{\frac{k_g}{k_s} + \left( \frac{1 - \sqrt{\epsilon}}{\sqrt{\epsilon}} \right)}} = k_s \cdot f(\epsilon, k_s^*). \quad (12)$$

In the limits of  $\epsilon \rightarrow 0$  and  $\epsilon \rightarrow 1$ , corresponding to pure solid and pure gas phase, respectively, Eq. 12 provides the following results:  $\lim_{\epsilon \rightarrow 0} k_{rs} = k_s$ ,  $\lim_{\epsilon \rightarrow 1} k_{rs} = k_g$ , which preliminarily prove its physical consistency.

According to Eq. 12, the effective radial conductivity of monoliths with square cells is obtained by multiplying the solid conductivity by a factor that depends primarily on the void fraction, and to a minor extent, on the gas-to-solid conductivity ratio. In line with the different mechanism of radial heat transfer, such a dependence markedly differs from those reported for packed-bed reactors. Indeed in monolith reactors heat transmission in the transverse direction occurs only by static conduction, since convective heat transfer, which plays a dominant role in packed beds, is prevented by the segregated flow pattern of the gas phase.

In Figure 2  $f(\epsilon, k_s^*)$  is plotted as a function of  $k_s^*$ , with  $\epsilon$  as a parameter. Asymptotic values are already approached for solid conductivities close to those of ceramic supports ( $k_s^* = 50$ ). Accordingly, the static gas-phase conductivity can be neglected in metallic monoliths, but plays some role in ceramic monoliths with high open frontal areas. The effective

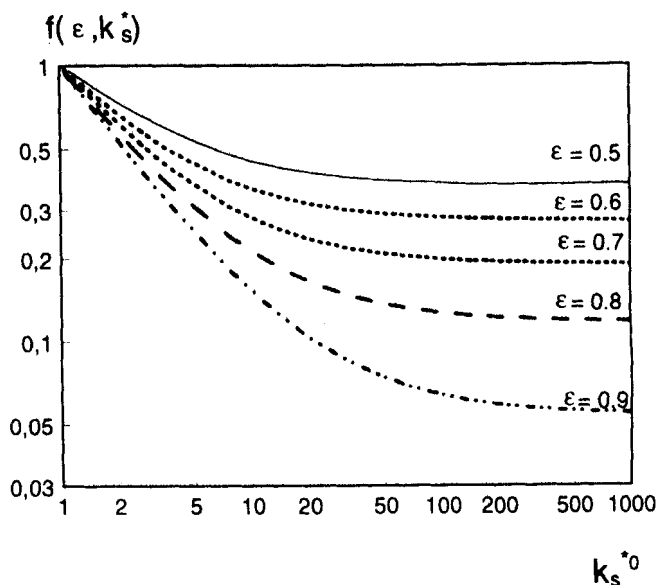


Figure 2. Dependence of the effective radial-to-solid conductivity ratio on  $k_s^*$  and  $\epsilon$ .

radial conductivity markedly decreases with increasing  $\epsilon$ , varying from 0.35 to 0.035 times the solid conductivity for  $\epsilon$  growing from 0.5 to 0.9.

The procedure just described with reference to a simple square geometry can be extended to different channel shapes and also to account for the effect of the active ceramic coating of typical monolith catalysts. As an example we provide the following expression for monoliths with isosceles triangular cells:

$$k_{rs} = k_s \cdot \frac{\cos \alpha + \frac{l}{4w} \cdot \sin \alpha}{\cos \alpha + \frac{l}{4w} + \left( \frac{l}{4w} \right)^2 \cdot \sin \alpha}, \quad (13)$$

with symbols explained in the Notation section.

Notably, this procedure requires no geometrical reconfiguration of the monolith, which is a major drawback of published discrete models. In principle, derivation of expressions for the effective radial conductivity may require some geometrical approximation when dealing with more complex channel shapes. However, once such an expression is available, actual geometrical parameters of the monolith (e.g., open frontal area and specific geometric surface) can be used with no lack of physical consistency of the model.

### Discrete model

The discrete model of the monolith reactor used herein has already been described elsewhere (Tronconi et al., 1994). Briefly, it implements a preliminary reconfiguration of the actual monolith matrix into an equal number of square channels arranged in  $N$  concentric rings to secure circular symmetry, according to Kolaczowski et al. (1988). For each single channel in the  $i$ th ring ( $i = 1, \dots, N$ ) the model consists of a differential gas-phase energy balance, a differential solid-phase energy balance, and a continuity relationship at the

gas–solid interface. This results in a differential-algebraic system of  $3N$  equations whose solution provides the axial temperature profiles of the gas phase, of the gas–solid interface, and of the solid wall of each channel along the radial coordinate of the reconfigured monolith matrix.

## Numerical Methods

The method of numerical solution of the model equations is an outstanding argument in favor of continuous models. In fact, discrete models impose a numerical grid for discretization of the temperature profiles that is intrinsically connected to the physical structure of the monolith. This results in a heavy finite difference scheme with a constant grid mesh. Typically, the number of grid points is a multiple of the number of the channel rings in the reconfigured monolith geometry, and such a number is often very large. On the other hand, the governing equations of continuous models consist of a set of partial differential equations (PDEs) with boundary conditions. The equation coefficients do depend on microscale geometry (i.e., on the geometry of the unit cell), but the numerical method of solution of the PDEs is completely decoupled from the microscale geometry. Consequently more efficient numerical methods than those imposed by the nature of the discrete model can be adopted. Orthogonal collocations based on symmetric Jacobi polynomials (Finlayson, 1980) have been used herein for discretization of radial temperature profiles over the monolith cross section: six to nine collocation points were generally sufficient to achieve convergence also in the case of monoliths consisting of tens (hundreds) of channel rings. Problems and methods concerning axial integration are equivalent for discrete and continuous models. Again, orthogonal collocations have been adopted herein for solution of the boundary-value problem generated by taking axial heat conduction into account.

## Comparison of Discrete and Continuous Monolith Models

Based on a parametric analysis, simulation results of continuous and discrete models have been compared in order to rate the adequacy of the continuous model in predicting the heat-transfer properties of the monolith matrix. By inspection of the dimensionless equations of the continuous model the following governing parameters are apparent:  $\epsilon$ ,  $L^*$ ,  $k_s^*$ ,  $Pe'$ ,  $D^*$ ,  $T_{ext}^*$ , and  $Nu$ . Investigation ranges have been derived from those reported in Table 1 for geometrical, physical, and operating characteristics of monolith catalysts. In line with the fundamental aim of this work, wider parametric ranges than those of practical interest have been considered.

The global heat flux exchanged between the monolith matrix and the flowing gas has been chosen as the relevant index in our comparative analysis for the following reasons: (1) it is an integral variable of practical importance, which is also obviously very sensitive to the heat-transfer properties of the monolith; and (2) an integral index seems more suitable for a parametric comparison than local ones, such as temperature profiles.

Significant percentage differences between the global heat fluxes predicted by the continuous and by the discrete monolith models have been computed at low values of the parameters  $k_s^*$ ,  $1/Pe'$ ,  $L^*$ , and  $(1 - \epsilon)$ . On incrementing all four pa-

**Table 1. Explored Ranges of Geometrical, Physical, and Operating Parameters of Monolith Catalysts**

Open frontal area ( $\epsilon$ )	0.1–0.9
Monolith pitch ( $m$ )	$1-9 \cdot 10^{-3}$ m
Monolith length ( $L$ )	0.05–5 m
Monolith diameter ( $D$ )	0.04–0.9 m
Thermal conductivity of the solid ( $k_s$ )	0.14–100 W/(m·K)
Specific mass-flow rate ( $G$ )	0.1–5 kg/(m <sup>2</sup> ·s)
Nusselt number ( $Nu_{ex}$ )	0.3–30
External wall to gas inlet temperature ratio ( $T_{ext}^*$ )	0.3–3

rameters, however, the predictions of the two models asymptotically converge, the calculated absolute percentage difference rapidly decreasing to negligible values. It has been verified that small percentage differences between predictions of the two models correspond to practically equivalent radial  $T$ -profiles. For example, Figure 3 illustrates the influence of  $k_s^*$  on the index for model comparison. On the other hand, simulation results indicate that  $D^*$ ,  $T_{ext}^*$ , and  $Nu$  do not affect significantly the deviations between continuous and discrete models over a wide range of values.

Note that the continuous and the discrete models agree within a few percentage points in the parametric regions corresponding to effective heat transfer from external wall to inner flowing gas. On the other hand, the predictions of the two models always diverge at conditions that correspond to low heat-transfer rates. In fact, according to Eq. 12 monoliths with low solid conductivities and high open frontal areas exhibit a poor effective radial conductivity, whereas short monolith lengths and high  $Pe'$  values result in small residence times, which do not allow for an effective heating of the gas stream. In terms of radial temperature profiles, such conditions correspond to small penetration depths of the heat flux. Figure 4 shows the radial  $T$ -profiles calculated by the continuous model for a typical set of parameters associated

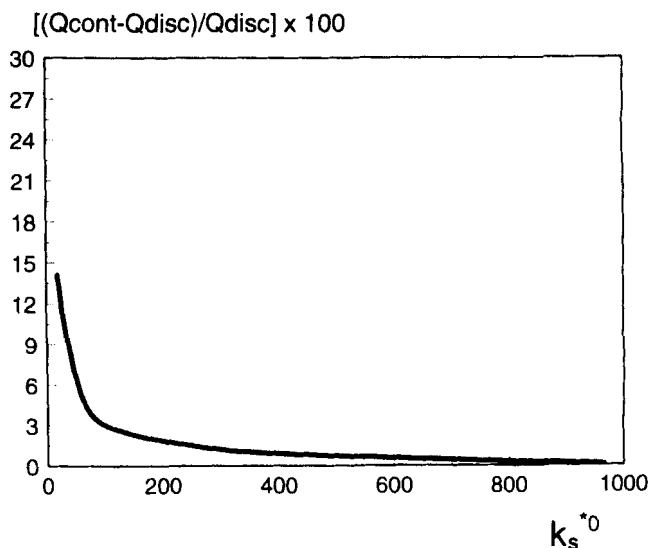


**Figure 3. Percentage difference of exchanged global heat flux calculated by continuous and discrete models as a function of  $k_s^*$ .**

Other parameter values:  $\epsilon = 0.7$ ;  $Pe'^0 = 202$ ;  $L^* = 40$ ;  $T_{ext}^* = 1.76$ ;  $D^* = 40$ .

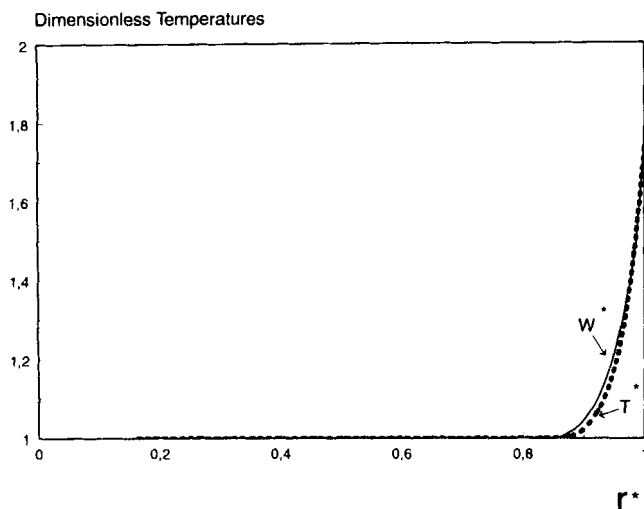


**Figure 4. Calculated radial profiles of dimensionless solid and gas temperatures.**

Parameter values:  $\epsilon = 0.7$ ;  $k_s^* = 5.4$ ;  $Pe'^0 = 202$ ;  $L^* = 40$ ;  $T_{ext}^* = 1.76$ ;  $D^* = 40$ .

with wide discrepancies between predictions of the continuous and of the discrete models: low heat-transfer rates result in steep radial temperature gradients confined in a narrow region close to the external monolith wall. The finite difference scheme with constant grid mesh (step = channel pitch) associated with the discrete model is likely to fail in representing accurately such steep profiles. Consequently, the observed deviations between the two models originate from the poor efficiency of the numerical procedure intrinsic to the discrete-model approach. In principle a more detailed discretization could also be adopted to secure an accurate solution under such critical conditions. However, this would require a revision of the model equations, and would result in a drastic enhancement of the computational duty owing to the geometrically constrained solution grid. For instance, the discrete model of the monolith structure proposed by Kolackowski and coworkers (1988) considers two temperatures of the solid phase in each annular ring, namely, the web wall and the ring wall temperature, rather than the single temperature of our simple discrete approach. Such a discretization may secure an improved convergence for some critical values of the model parameters, but it also brings about an important increase in the number of independent model variables. On the other hand, the continuous approach allows the extent of numerical discretization along the radial coordinate to vary without affecting the structure of the model equations at all: in our computations, a greater number of collocation points (up to nine) was used to achieve a converged solution of the continuous model for conditions corresponding to strong  $T$ -gradients.

In summary, the present continuous model of heat transfer in monolith matrices appears at least as physically reliable as the conventional discrete one, but definitely more robust, flexible, and effective from the numerical point of view.

## Conclusions

A novel, physically consistent expression for the effective radial thermal conductivity of the connected solid phase in

monolith matrices has been derived for square and triangular channels from the analysis of the heat-transfer mechanisms in the monolith cells. A related two-dimensional heterogeneous pseudocontinuous steady-state model of heat transfer in monolith structures has been developed and systematically compared with a conventional model, based on a discrete approach. The discrete and the continuous models agree closely over a wide parametric field, which proves the intrinsic adequacy of the continuous approach. However, the continuous model allows for remarkable savings in computational effort. Deviations between the two types of models are observed under parametric conditions associated with steep radial temperature gradients, where the numerical approximation inherent to the discrete model becomes unacceptable: in such cases, the solutions generated by the continuous model are expected to be more reliable. In fact, a major merit of the continuous approach is to decouple the model equations from the numerical methods for their solution. In principle as well in practice, this results in a greater computational efficiency, but also in a better accuracy when critical situations are encountered. Extension of the same approach to modeling of monolith catalysts with chemical reactions is straightforward.

## Acknowledgments

Financial support from MURST-Roma is gratefully acknowledged.

## Notation

- $A_c$  = monolith unit cell surface in the direction perpendicular to radial heat flow,  $m^2$
- $C_p$  = specific heat,  $J \cdot kg^{-1} \cdot K^{-1}$
- $d$  = length of square-channel side,  $m$
- $D^* = D/m$  = dimensionless monolith diameter
- $k^* = k/k_g$  = dimensionless thermal conductivity
- $l$  = length of the triangular cell basis,  $m$
- $L^* = L/m$  = dimensionless monolith length
- $Nu = (h \cdot d)/k_g$
- $Pe' = (G \cdot m \cdot C_p)/k_g$  = modified Peclet number
- $\dot{Q}$  = heat flux,  $W$
- $r$  = radial coordinate,  $m$
- $r^* = 2r/D$  = dimensionless radial coordinate
- $s_c$  = cell length along the heat flow direction,  $m$
- $T$  = gas temperature,  $K$
- $T^* = T/T_g^0$  = dimensionless gas temperature
- $T_{ext}^*$  = dimensionless external wall temperature
- $w$  = half wall thickness in triangular channels,  $m$
- $W$  = solid temperature,  $K$
- $W^* = W/T_g^0$  = dimensionless solid temperature
- $z$  = axial coordinate,  $m$
- $z^* = z/L$  = dimensionless axial coordinate

## Greek letters

- $\alpha$  = basis angle of triangular channels
- $\delta$  = wall thickness in square channels,  $m$
- $\epsilon$  = open frontal area

## Subscripts and superscripts

- 0 = inlet conditions
- cont = continuum model
- disc = discrete model
- g = gas properties
- s = solid properties

## Literature Cited

- Aris, R., "De Exemplo Simulacrorum Continuum Discritalumque," *Arch. Rat. Mech. Anal.*, **70**, 203 (1979).

- Bauer, R., and E. U. Schlunder, "Effective Radial Conductivity of Packing in Gas Flow. Part I. Convective Transport Coefficient," *Int. Chem. Eng.*, **18**, 181 (1978).
- Cybulski, A., and J. A. Moulijn, "Monoliths in Heterogeneous Catalysis," *Catal. Rev. Sci. Eng.*, **36**(2), 179, and references therein (1994a).
- Cybulski, A., and J. A. Moulijn, "Modelling of Heat Transfer in Metallic Monoliths Consisting of Sinusoidal Cells," *Chem. Eng. Sci.*, **49**, 19 (1994b).
- Finlayson, B. A., *Nonlinear Analysis in Chemical Engineering*, McGraw-Hill, New York (1980).
- Flytzani-Stephanopoulos, M., G. E. Voecks, and T. Charng, "Modelling of Heat Transfer in Non-adiabatic Monolith Reactors and Experimental Comparison of Metal Monoliths with Packed Beds," *Chem. Eng. Sci.*, **41**, 1203 (1986).
- Grigull, U., and H. Tratz, "Thermischer Einlauf in Ausgebildeter Laminarer Rohrströmung," *Int. J. Heat Mass Transfer*, **8**, 669 (1965).
- Kolaczowski, S. T., P. Crumpton, and A. Spence, "Modelling of Heat Transfer in Non-adiabatic Monolithic Reactors," *Chem. Eng. Sci.*, **43**, 227 (1988).
- Liu, Y., "Equivalent Continuum Models for Nonadiabatic Monolith Catalytic Reactors," PhD diss., Rice Univ., Houston, TX (1975).
- Stewart, W. E., K. L. Levien and M. Morari, "Simulation of Fractionation by Orthogonal Collocation," *Chem. Eng. Sci.*, **40**, 409 (1985).
- Tronconi, E., M. Bassini, P. Forzatti, and D. Carmello, "Design of Monolith Catalysts for Strongly Exothermic Reactions under Nonadiabatic Conditions," *Preparation of Catalysts: VI. Scientific Bases for the Preparation of Heterogeneous Catalysts*, G. Poncelet, J. Martens, B. Delmon, P. A. Jacobs, and P. Grange, eds., Elsevier, Amsterdam, p. 765 (1995).
- Zygourakis, K., "Transient Operation of Monolith Catalytic Converters: A Two-Dimensional Reactor Model and the Effects of Radially Nonuniform Flow Distributions," *Chem. Eng. Sci.*, **44**, 2075 (1989).

*Manuscript received Apr. 24, 1995, and revision received Dec. 6, 1995.*